Process Optimization of WEDM for Machining of Aluminum (6063)/Graphite Metal Matrix Composites

Tejas Pramod Naik, Promod Kumar Patowari, Kassahun Gashu Melese, Ram Singh Rana, Inderdeep Singh, and Apurbba Kumar Sharma

1 Introduction

In the field of cutting edge assembling and designing, composite materials are now playing an important role. Due to increasing demand from technological advancements in the field of aerospace, aircraft, and automobile industries, there is a need for smart and advanced materials [1]. Metal matrix composite (MMC) has always been attractive to researchers as a substitution for pure metallic materials because of its low specific gravity without compromising its strength. It has been conceivable to create novel composite materials with improved physical and mechanical properties in light of countless investigations occurring into the basic idea of materials and a superior comprehension of their structure–property relationship [2]. The traditional way of

---

T. P. Naik (✉) · I. Singh · A. K. Sharma
Design Innovation Center, Indian Institute of Technology Roorkee, Roorkee, Uttarakhand 247667, India
e-mail: tejasnit@gmail.com

I. Singh
e-mail: inderdeep.singh@me.iitr.ac.in

A. K. Sharma
e-mail: aks@me.iitr.ac.in

P. K. Patowari
Department of Mechanical Engineering, National Institute of Technology Silchar, Assam 788010, India
e-mail: ppatowari@yahoo.com

T. P. Naik · K. G. Melese · R. S. Rana · I. Singh · A. K. Sharma
Mechanical and Industrial Engineering Department, Indian Institute of Technology Roorkee, Roorkee, Uttarakhand 247667, India
e-mail: kassahung28@yahoo.com

R. S. Rana
e-mail: ramsingh.mech17@gmail.com

P. K. Rakesh et al. (eds.), *Advances in Engineering Design*, Lecture Notes in Mechanical Engineering, https://doi.org/10.1007/978-981-33-4018-3_8

machining of these advanced materials is difficult; therefore, to overcome these challenges, wire-EDM, which is a non-conventional process, is gaining importance these days. WEDM is a thermo-electrical procedure in which material is removed from the workpiece by the arrangement of discrete sparks among workpiece and wire. While machining, there is no physical contact between tool and workpiece [3]. Therefore, the tool in this process is not eroded, and the finish on the workpiece surface is also very high compared to any conventional machining process. The schematic picture of WEDM appears in Fig. 1. This paper considers four control parameters, in particular, pulse on time (T_{on}) (μs), pulse off time (T_{off}) (μs), peak current (I_p) (A), and table feed (S) (μm/s), while rest of the parameters are kept steady. Taguchi L16 symmetrical cluster has been intended to carry out the investigation study [4]. Yigezu et al. [5] have investigated the ceramic particle reinforced aluminum composites. It was reported that for the fabrication of the metal matrix composites, stir casting route is cost effective and straightforward. Mazahery and Shabani [6] have researched the mechanical properties of B_4C fortified A356 composite. It was discovered that the porosity, rigidity, and hardness are higher than the Al compound and increment with an increase in the B_4C content. Rahman et al. [7] have determined the impact of EDM input responses on the MRR of titanium (Ti) alloy. They have concluded that current and T_{on} were the most influencing parameters affecting MRR. Liu et al. [8] utilized wire electrochemical discharge machining to study the machining characteristics of Al_2O_3/aluminum composites. They found that material removal rate increases with high current.

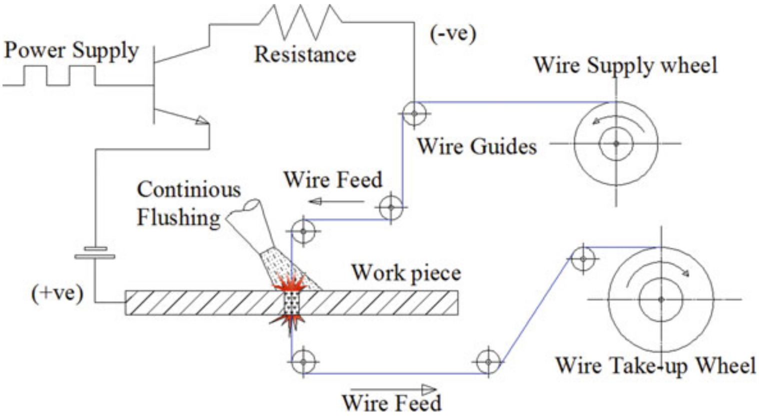

Fig. 1 Schematic diagram of CNC WEDM [9]

Fig. 2 Wire electrical discharge machine

2 Experimental Investigations

2.1 Materials and Method

The aluminum (6063) rods supplied by Madhab and Company, Kolkata, West Bengal, India, and Graphite powder of mesh size 60 was used for the fabrication of metal matrix composites. The investigations were done on a CNC WEDM machine located at NIT Silchar (Make: Ratnaparkhi Electronics (I) Pvt Ltd.) which is shown in Fig. 2. The dielectric fluid used for the study was de-ionized water which is continuously flushed at the machining zone to remove the debris produced during the machining.

2.2 Design of Experiments

Input parameters, for example, pulse on time (T_{on}), pulse off time (T_{off}), peak current (I_{P}), and table feed (S) utilized in this investigation study are given in Table 1. Each factor is examined at four levels to decide the ideal settings for the WEDM procedure. These parameters and their levels have been picked dependent on the Taguchi investigation for the tests to be directed. The Design of experiment (DOE) with Taguchi's L16 symmetrical cluster dependent on four information parameters having four distinct levels appears in Table 2.

Table 1 Input parameters

Symbol	Input parameters	Unit	Value 1	Value 2	Value 3	Value 4
T_{on}	Pulse on time	μs	25	35	45	55
T_{off}	Pulse off time	μs	8	10	12	14
I_P	Peak current	A	2	3	4	5
S	Table speed	μm/s	46.70	55.60	60.00	69.90

Table 2 Taguchi L16 design of experiment

Exp. no	T_{on} (μs)	T_{off} (μs)	I_p (A)	S (μm/s)
1	25	8	2	46.7
2	25	10	3	55.6
3	25	12	4	60.0
4	25	14	5	69.9
5	35	8	3	60.0
6	35	10	2	69.9
7	35	12	5	46.7
8	35	14	4	55.6
9	45	8	4	69.9
10	45	10	5	60.0
11	45	12	2	55.6
12	45	14	3	46.7
13	55	8	5	55.6
14	55	10	4	46.7
15	55	12	3	69.9
16	55	14	2	60.0

2.3 Experimental Results

The tool utilized during the tests was a brass wire of 0.22 mm diameter. The workpiece picked was a composite of measurements 30 mm × 24 mm × 5 mm. The cutting length in all the tests was fixed; equivalent to 5 mm. Dielectric utilized was deionized water, which is flushed continuously to the machining zone to divert the debris particles. The whole arrangement of investigations has been completed three times. While performing out each arrangement of analysis, values for MRR and CR have been determined, and KW was seen on a microscope. Finally, the average estimations of MRR, CR, and KW have been determined and are given in Table 3. Figure 3a–d shows the figure of a composite workpiece reinforced with graphite with two distinctive wt. percentage (5 and 10%) alongside its optical pictures of kerf width.

The kerf width (in μm), of each experimental, has been seen by the metallurgical microscope model number DM 2500M (Make: Leica). The material removal rate

Table 3 Values of response measures using WEDM in Al-Graphite (5 and 10%) composite

Exp. no	5% by wt			10% by wt		
	MRR (mg/s)	Cutting rate (µm/s)	Kerf width (µm)	MRR (mg/s)	Cutting rate (µm/s)	Kerf width (µm)
1	0.1874	46.30	420.65	0.3248	45.87	413.51
2	0.1765	51.02	427.05	0.3316	52.63	445.03
3	0.3149	57.47	443.84	0.4695	60.98	474.7
4	0.3197	70.42	441.62	0.5873	70.42	452.45
5	0.3544	55.56	431.61	0.4107	59.52	452.45
6	0.4289	69.44	428.23	0.5813	66.67	445.03
7	0.4413	45.87	493.95	0.3714	47.62	482.12
8	0.2917	52.08	471.53	0.3691	51.55	489.54
9	0.4726	68.49	475.01	0.5600	66.67	470.99
10	0.4145	60.24	485.08	0.4488	59.52	519.21
11	0.3908	52.08	444.88	0.3626	50.51	437.62
12	0.2563	44.64	452.01	0.3914	47.62	489.54
13	0.3447	52.63	496.00	0.4583	52.08	519.21
14	0.3176	47.17	476.11	0.4355	45.45	500.66
15	0.6108	66.67	456.93	0.6014	70.42	470.99
16	0.2732	60.24	442.58	0.4512	58.14	429.07

(mg/s) is calculated utilizing equation 1.

$$\mathrm{MRR} = \frac{\text{weightloss}}{\text{machining time}} \tag{1}$$

where weight loss = difference between the initial and final weights of the composite sample.

Cutting rate (µm/s) is determined to utilize equation 2.

$$\mathrm{CR} = \frac{\text{Cuttinglength(fixed5mm)}}{\text{machining time}} \tag{2}$$

For the most part, OEC is performed while the clashing measure is available in the investigation, and it is calculated using equation 3 [9]. As in this investigation, the requirement is of having kerf width of the slot as minimum and MRR and cutting rate as maximum, so equal weightage has been given to all the output responses, i.e., 33.33%.

$$\mathrm{OEC} = \left(\frac{X - X\min}{X\max - X\min} \times Wx\right) + \left(\frac{Y - Y\min}{Y\max - Y\min} \times Wy\right)$$

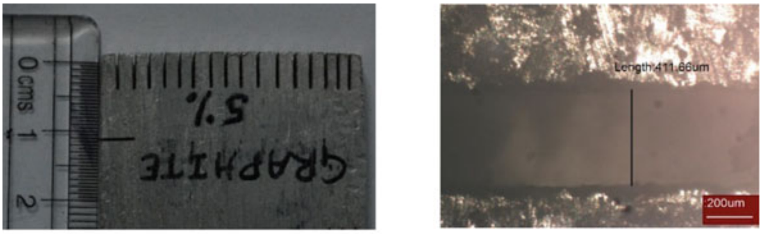

a). Machined Sample Al/5% Graphite Composite

b). Optical microscopic image of cut (at 100X magnification) by exp. No. 1

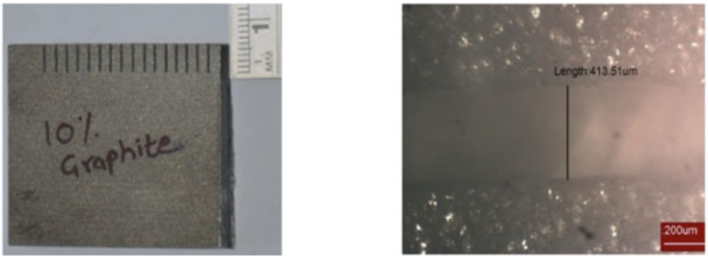

c). Machined Sample Al/10% Graphite Composite

d). Optical microscopic image of cut (at 100X magnification) by exp. No. 1

Fig. 3 Machined composites and microscopic image

$$+\left((1-\frac{Z-Z\text{min}}{Z\text{max}-Z\text{min}})\times Wz\right) \tag{3}$$

where

X, Y, and Z = test value of MRR, CR, and KW respectively.
X_{max}, Y_{max}, and Z_{max} = best values of MRR, CR, and KW respectively.
X_{min}, Y_{min}, and Z_{min} = worst values of MRR, CR, and KW respectively.
W_x, W_y, and W_z = equal weightage, i.e., 33.33%.

3 Results and Discussion

Figure 4 shows the impact of T_{on}, T_{off}, I_{p}, and S on MRR. It is obvious from the figure that MRR increases with an increase in T_{on} this is a direct result of an increasingly large number of pulses striking the workpiece that progressively removes material

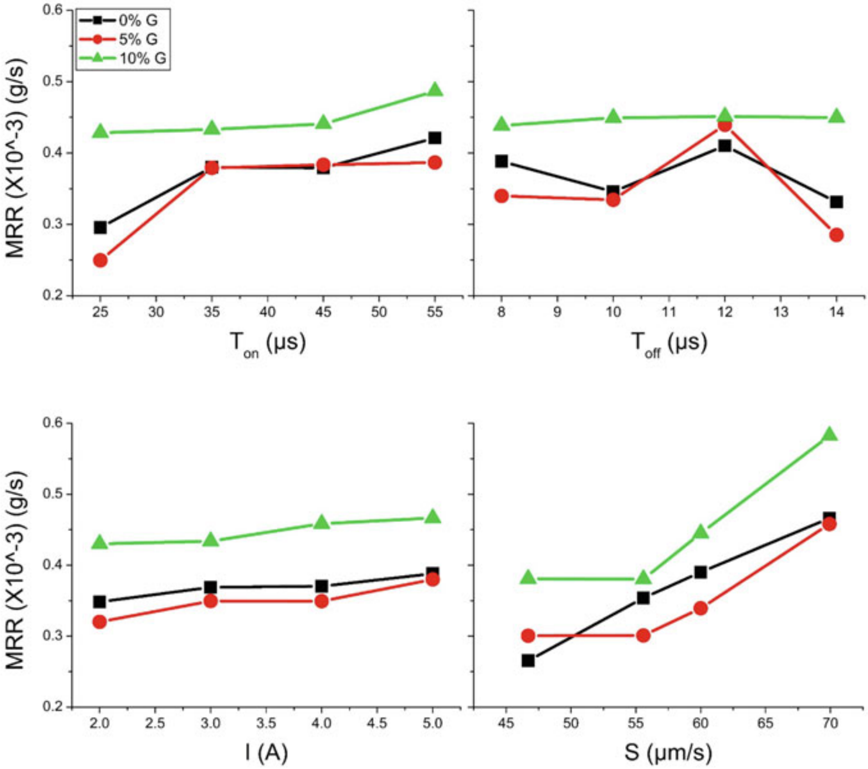

Fig. 4 Effect of input parameters on MRR for different reinforcing graphite content

and prompts higher MRR. If T_{on} is high, more time will be provided for the material to receive heat, to get vaporized, which will increase the MRR. However, as T_{on} decreases, MRR decreases because the pulses will strike the workpiece for less amount of time, and suddenly T_{off} will start, which will not allow the vaporization of the material. As I_p increase, more energy is supplied, which increases MRR. Moreover, it is seen that with increasing S, MRR increases because of the rapid movement of the table.

Figure 5 shows the impact of T_{on}, T_{off}, I_p, and S on cutting rate. It is obvious from the figure that S is a most important factor when contrasted with other responses. As S increases, the cutting rate increases due to the quick movement of the table. Also, it is seen that the cutting rate for pure aluminum is more compared to the composite material because the graphite particles which are used as reinforcement has a higher melting point, and so it obstructs the rate of cutting as it takes time to melt the graphite particle. Likewise, no significant distinction is seen in the cutting rate for both 5 and 10% graphite-reinforced composites.

Figure 6 shows the impact of T_{on}, T_{off}, I_p, and S on KW. By and large, it is obvious from figure that with an increase in T_{on}, kerf width increases since progressively

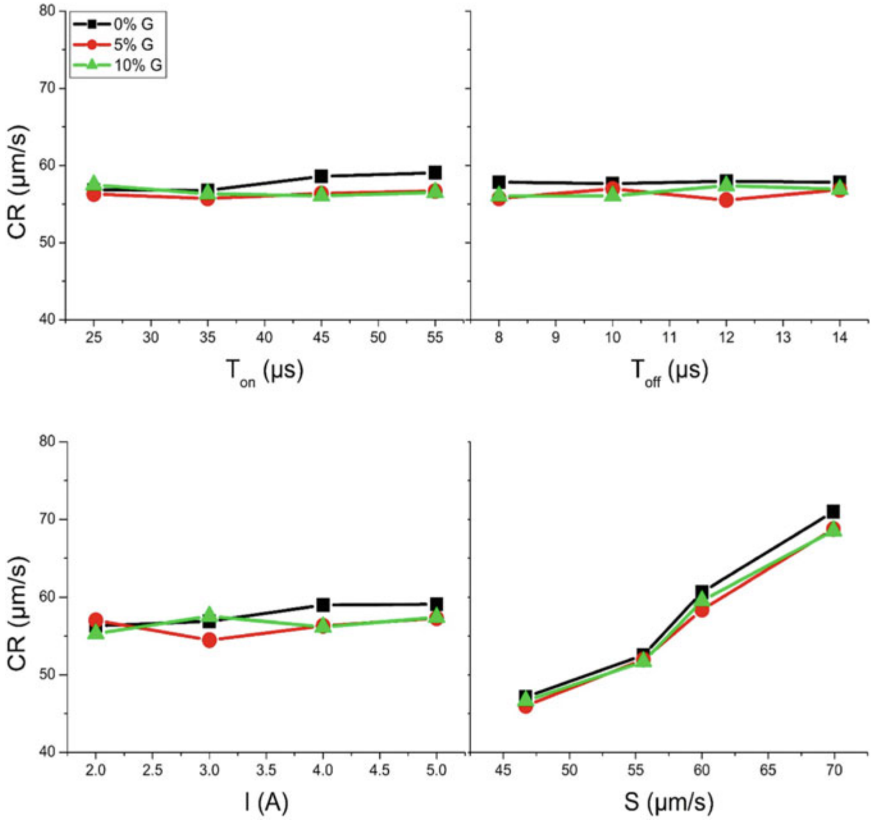

Fig. 5 Effect of input parameters on cutting rate for different reinforcing graphite content.

more material removal prompts higher KW. However, T_{off} does not significantly influence the KW. Because of increase in I_{p}, kerf width increases since more energy is provided, which prompts a higher concentration of release energy in the spark gap which brings about more significant cavity development. However, an increase in S decreases the kerf width as the table moves at a faster rate. It is observed that while machining in the composite material, brass wire (tool) faces graphite particles in between, which acts like a boundary for the wire while machining, thus results in narrow kerf width as compared to kerf width in the unreinforced material.

Table 4 depicts the OEC values for each experimental run, and it is found out that maximum OEC in case of Al-5% Graphite is 81.42, and in the case of Al-10% Graphite is 86.42.

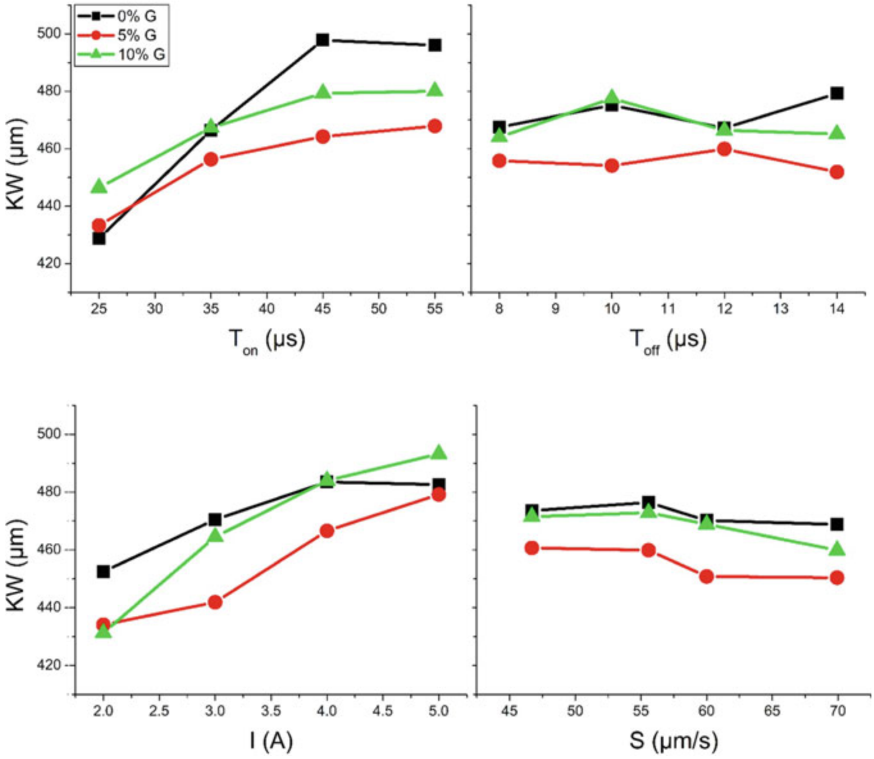

Fig. 6 Effect of input parameters on kerf width for different reinforcing graphite content.

3.1 Confirmation Test

Based on the OEC values, the graph has been plotted using Minitab software, and the optimum parametric conditions have been observed. Based on these conditions, experiments were again conducted three times, and the average values of the MRR, CR, and KW have been obtained. The predicted OEC value for the optimal condition is obtained using Minitab software. The actual OEC value for the optimum values of the output conditions has been calculated using the same equation 3. This actual OEC value and the predicted value are compared, and the % deviation is found out, which is given in Table 5.

4 Conclusions

The key results are summarized as follows:

Table 4 Overall evaluation criteria

Exp. no	Al-5% Graphite	Al-10% Graphite
1	36.31	33.89
2	38.75	33.79
3	50.29	52.20
4	68.38	*86.02*
5	56.25	50.19
6	*81.42*	82.62
7	22.82	20.21
8	29.29	22.83
9	62.85	71.87
10	43.26	33.73
11	48.68	37.03
12	25.58	20.28
13	23.24	24.94
14	22.90	19.19
15	79.09	81.87
16	51.22	60.59

Table 5 Confirmation test results

Composites	Observed OEC	Predicted OEC	% Deviation
Al-5% Graphite	87.86	87.18	0.77
Al-10% Graphite	87.45	96.32	10.14

- During the machining of Al-5% Graphite composites, the highest MRR was found to be 0.6108 mg/s, and the lowest MRR was 0.1765 mg/s. The highest cutting rate was found to be 70.42 μm/s, and the lowest was found to be 44.64 μm/s. The minimum kerf width obtained was 420.65 μm, and the largest was 496.00 μm.
- The optimum parametric conditions after the application of OEC in the case of 5% reinforced graphite composite were found to be $T_{\text{on}} = 25$ μs, $T_{\text{off}} = 12$ μs, $I_{\text{p}} = 2$ A, and $S = 69.9$ μm/s. After performing OEC, the % deviation between observed and predicted OEC was found to be 0.77%.
- However, in Al-10% Graphite composites, the highest MRR was found to be 0.6014 mg/s, and the lowest MRR was 0.3248 mg/s. The highest cutting rate was found to be 70.42 μm/s, and the lowest was found to be 45.45 μm/s. The minimum kerf width obtained was 413.51 μm, and the largest was 519.21 μm.
- The optimum parametric condition after the application of OEC in the case of 10% reinforced graphite composite was found to be $T_{\text{on}} = 25$ μs, $T_{\text{off}} = 12$ μs, $I_{\text{p}} = 2$ A, and $S = 69.9$ μm/s. After performing OEC, the % deviation between observed and predicted OEC was found to be 10.14%.

Acknowledgements The author, Tejas Pramod Naik, gratefully acknowledges the Design Innovation Center (DIC), Ministry of Human Resource and Development (MHRD), Government of India, for providing fellowship for the Ph.D. work.

References

1. Surappa MK (2003) Aluminium matrix composites: challenges and opportunities. Sadhana 28:319–334
2. Kala H, Mer KKS, Kumar S (2014) A review on mechanical and tribological behaviors of stir cast aluminum matrix composites. Proc Mater Sci 6:1951–1960. https://doi.org/10.1016/j.mspro.2014.07.229
3. Ramakrishnan R, Karunamoorthy L (2006) Multi response optimization of wire EDM operations using robust design of experiments. Int J Adv Manuf Technol 29:105–112. https://doi.org/10.1007/s00170-004-2496-6
4. Mahapatra SS, Patnaik A (2006) Parametric optimization of wire electrical discharge machining (WEDM) process using Taguchi method. J Brazilian Soc Mech Sci Eng 28:422–429. https://doi.org/10.1590/S1678-58782006000400006
5. Yigezu BS, Jha PK, Mahapatra MM (2013) The key attributes of synthesizing ceramic particulate reinforced Al-based matrix composites through stir casting process: a review. Mater Manuf Process 28:969–979. https://doi.org/10.1080/10426914.2012.677909
6. Mazahery A, Shabani MO (2012) Mechanical properties of squeeze-cast A356 composites reinforced with B 4C particulates. J Mater Eng Perform 21:247–252. https://doi.org/10.1007/s11665-011-9867-6
7. Rahman MM, Khan MAR, Kadirgama K (2010) Modeling of material removal on machining of Ti-6Al-4V through EDM using copper tungsten electrode and positive polarity. World Acad Sci Eng Technol 71:576–581
8. Liu JW, Yue TM, Guo ZN (2009) Wire electrochemical discharge machining of Al_2O_3 particle reinforced aluminum alloy 6061. Mater Manuf Process 24:446–453. https://doi.org/10.1080/10426910802714365
9. Naik TP, Debnath T, Patowari PK (2018) Machinability study on German silver using wire-EDM. AIP Conf Proc 1998:1–8. https://doi.org/10.1063/1.5049100